

General Higher Order Extension to the Quiet Direct Simulation Method

Y.-J. Lin^a, M. R. Smith^b, H. M. Cave^{a,c}, J.-C. Huang^d, J.-S. Wu^{a,b*}

^a*National Chiao Tung University, Department of Mechanical Engineering, HsinChu, Taiwan*

^b*National Center for High-performance Computing, HsinChu, Taiwan*

^c*University of Canterbury, Department of Mechanical Engineering, New Zealand*

^d*National Taiwan Ocean University, Department of Merchant Marine, Taiwan*

Abstract. Presented is the multi-dimensional extension of the Quiet Direct Simulation (QDS) method to general, higher order spatial accuracy. Due to the true directional nature of QDS, where volume-to-volume fluxes are computed as opposed to fluxes at cell interfaces, a volumetric reconstruction is required. In this approach, the conserved quantities are permitted to vary (according to a polynomial expression) across all simulated dimensions. Prior to flux computation, QDS particles are introduced using properties based on weighted moments taken over the polynomial reconstruction of conserved quantity fields. The resulting flux expressions are shown to exactly reproduce existing 2nd order extensions (for one-dimensional flows) while providing means for true multi-dimensional reconstruction and general higher order extensions. Here we will show a typical comparison among different spatial order extensions of QDS and other WENO (5th order accurate) based numerical scheme. The extension is demonstrated up to 5th order spatial accuracy and is shown to be comparable to or more accurate than the other higher order schemes.

Keywords: QDSMC, QDS, Euler Equations, TDEFM, CFD, The Kinetic Theory of Gases.

PACS: 02.50.Cw, 02.60.Cb, 02.70.Dh, 05.20.Dd, 47.11.Df, 47.10.ad, 47.45.Ab, 47.40.Ki

INTRODUCTION

Since the development of DSMC (Direct Simulation Monte Carlo) by Bird [1], a large number of continuum kinetic theory based schemes have emerged. In 1980, Pullin proposed the Equilibrium Flux Method (EFM) as an analytical equivalent to the Equilibrium Particle Simulation Method (EPSM), which is a direct simulation method where particles are forced to assume the Maxwell-Boltzmann equilibrium velocity probability distribution function instead of performing collisions [2]. Later, Smith et al. proposed a general form of the EFM method known as the True Direction Equilibrium Flux Method (TDEFM) [3] which more accurately captures the transport mechanism employed by EPSM. Fluxes calculated by TDEFM represent the true analytical solution to the molecular free flight problem under the assumption of thermal equilibrium and uniformly distributed quantities.

Albright et. al. [4] previously developed a numerical scheme for the solution of the Euler Equations known as the Quiet Direct Simulation Monte Carlo (QDSMC). In this method, the integrals encountered in the TDEFM formulation are replaced by approximations using Gaussian numerical integration – effectively replacing the continuous velocity distribution function with a series of discrete velocities. The method was later renamed as the Quiet Direct Simulation (QDS) method due to the lack of stochastic processes and extended to 2nd order spatial accuracy [5]. The lack of complex mathematical functions results in a computationally efficient scheme with a performance higher than that of EFM while maintaining the advantages of true directional fluxes [5].

Due to the assumption of unrestricted motion during free flight, each of these solvers possess a large amount of (cell-sized based) numerical diffusion. To combat this dissipation, a common strategy employed in more conventional finite volume methods is higher order reconstruction of properties or fluxes. Macrossan [6] has applied EFM using higher order spatial extensions: later, Smith [7] attempted the analytical inclusion of gradients into true-direction, volume to volume fluxes only to find the complete analytical inclusion of gradient terms in the TDEFM flux expressions is impossible. In this paper, we extend the QDS algorithm to high-order reconstruction through the

polynomial, multidimensional reconstruction of conserved properties across each cell width. The net fluxes are computed through individual contributions of QDS particles computed by taking moments over the polynomial reconstruction. In order to ensure positivity, and following previous spatial accuracy extension, slope limiting functions are employed to ensure that non-physical oscillations are produced. The method is then applied to various one and two dimensional benchmark problems and compared to results obtained using a higher order WENO scheme [8].

NUMERICAL METHOD

Quiet Direct Simulation (QDS)

The normal random variable $N(0,1)$ is defined by the probability density:

$$p(x) = \frac{e^{-x^2/2}}{\sqrt{2\pi}} \quad (1)$$

Since fluxes formulated from kinetic theory are derived from moments of the distribution function, it is proposed that one can safely replace the moment of a distribution function with a discrete summation. Using Gaussian quadrature, the integral of equation (1) over its limits can be approximated by:

$$\int_{-\infty}^{\infty} \frac{e^{-x^2/2}}{\sqrt{2\pi}} f(x) dx \approx \sum_{j=1}^N w_j f(q_j) \quad (2)$$

where w_j and q_j are the weights and abscissas of the Gaussian quadrature (also known as the Gauss-Hermite parameters), N are the number of terms and $f(x)$ is unity. The abscissas are the roots of the Hermite polynomials which can be defined by the recurrence equation:

$$H_{n+1}(q) = 2qH_n - 2nH_{n-1} \quad (3)$$

where $H_{-1}=0$ and $H_0=1$. The weights can be determined from:

$$w_j = \frac{2^{n-1} n! \sqrt{\pi}}{n^2 [H_{n-1}(q_j)]^2} \quad (4)$$

The total flux of mass, momentum and energy from a one-dimensional source into a one-dimensional destination is given by the sum of individual flux contributions from each ‘‘particle’’:

$$F_{MASS} = \sum_{J=1}^N F_{MASS}^J \quad F_{MOM} = \sum_{J=1}^N F_{MOM}^J \quad F_{ENG} = \sum_{J=1}^N F_{ENG}^J \quad (5)$$

where F_{MASS}^J is the individual mass flux from particle J . Each of the individual contributions (with first order spatial accuracy) can be described by the expressions:

$$F_{MASS,J} = \frac{v_J \Delta t}{\Delta x} m_J \quad F_{MOM}^J = \frac{v_J \Delta t}{\Delta x} m_J v_J \quad F_{ENG}^J = \frac{v_J \Delta t}{\Delta x} m_J \left[\frac{1}{2} v_J^2 + \varepsilon_J \right] \quad (6)$$

where the particle mass m_J , particle velocity v_J and particle internal energy ε_J are:

$$m_J = \frac{\rho \Delta x w_J}{\sqrt{\pi}} \quad v_J = u + \sqrt{2} \sigma q_J \quad \varepsilon_J = \frac{(\xi - \Omega) \sigma^2}{2} \quad (7)$$

where ρ is the density, u is the bulk (or mean) flow velocity and $\sigma = (RT)^{0.5}$ in a given source cell or source region. The total number of degrees of freedom ξ is defined as $\xi = 2(\gamma - 1) - 1$ and Ω the number of simulated degrees of freedom ($\Omega = 1$ for one dimensional flows). In existing second order extensions of QDS, the values of ρ , u and σ employed in QDS particle initialization are taken from reconstructions based on linear variations. Despite fluxes being true direction in nature, the reconstruction performed by previous implementations are direction decoupled – i.e. a flux is computed through the product of (separate) fluxes previously computed (for 2D flow) in the x and y directions. The resulting reconstructed fluxes produce anomalies discussed in later sections of this report.

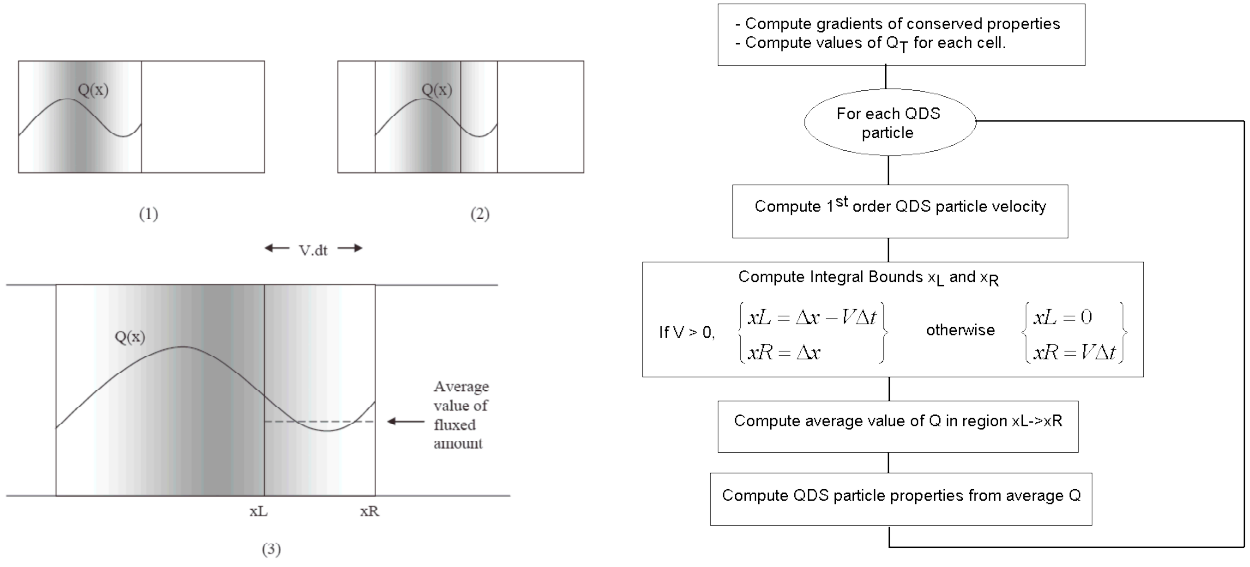


FIGURE 1. [Left] Polynomial construction of conserved quantity $Q(x)$ showing the average value of Q in the “source” region employed for particle property determination, [Right] Flowchart describing QDS particle computation with gradient inclusion.

1D Spatial Reconstruction and Implementation

In this investigation, the general extension to higher order in QDS (as shown in Figure1) is performed using a spatial reconstruction of the form:

$$Q(x) = Q_{eff} + \left(\frac{dQ}{dx}\right)(x - 0.5\Delta x) + \left(\frac{d^2Q}{dx^2}\right)\frac{(x - 0.5\Delta x)^2}{2} \dots + \left(\frac{d^{n-1}Q}{dx^{n-1}}\right)\frac{(x - 0.5\Delta x)^{n-1}}{(n-1)!} \quad (8)$$

where $Q(x)$ is the value of a conserved property (mass, momentum or energy) at a distance x from the left hand side of the cell and integer n indicates the order of the reconstruction. To ensure that the average value of $Q(x)$ over the entire cell width is equal to the existing (cell center) average (i.e. the first order value of $Q=Q_T$), the effective value of Q at the cell center Q_{eff} must be:

$$Q_{eff} = Q_T - \frac{\Delta x^2}{24}\left(\frac{d^2Q}{dx^2}\right) - \frac{\Delta x^4}{1920}\left(\frac{d^4Q}{dx^4}\right) \dots - \frac{2\Delta x^{n-1}}{n!}\left(\frac{1}{2}\right)^n\left(\frac{d^{n-1}Q}{dx^{n-1}}\right) \quad (9)$$

where n is assumed to be an odd number. Thus correction is only required when the scheme is third order ($n = 3$) accurate or higher, otherwise $Q_{eff} = Q_T$. The average value of conserved quantity successfully moving from the source cell into the destination cell (denoted by \bar{Q}) is:

$$\begin{aligned} \bar{Q} &= \frac{1}{(x_R - x_L)} \int_{x_L}^{x_R} Q(x) dx \\ &= Q_{eff} + \frac{1}{(x_R - x_L)} \left[\left(\frac{dQ}{dx}\right)\frac{(x_R - 0.5\Delta x)^2}{2} \dots + \left(\frac{d^{n-1}Q}{dx^{n-1}}\right)\frac{(x_R - 0.5\Delta x)^n}{n!} \right] \\ &\quad - \frac{1}{(x_R - x_L)} \left[\left(\frac{dQ}{dx}\right)\frac{(x_L - 0.5\Delta x)^2}{2} \dots + \left(\frac{d^{n-1}Q}{dx^{n-1}}\right)\frac{(x_L - 0.5\Delta x)^n}{n!} \right] \end{aligned} \quad (10)$$

where the “source region” is bound by x_R and x_L which are functions of the particle velocities. The mean values \bar{Q} are used to calculate particle properties, as described in Figure 1. Assigning the average conserved properties \bar{Q}_1, \bar{Q}_2 and \bar{Q}_3 as the mass, momentum and energy respectively, the resulting QDS particle properties for particle i are:

$$m_j = \frac{\bar{Q}_1 W_i}{\sqrt{\pi}} \quad v_j = \frac{\bar{Q}_2}{\bar{Q}_1} + \left[\frac{2R}{C_v} \left(\frac{\bar{Q}_3}{\bar{Q}_1} - \frac{1}{2} \left(\frac{\bar{Q}_2}{\bar{Q}_1} \right)^2 \right) \right]^{\frac{1}{2}} ABSC_i \quad \varepsilon_j = \frac{(\xi - \Omega)R}{2} \left(\frac{\bar{Q}_3}{\bar{Q}_1} - \frac{1}{2} \left(\frac{\bar{Q}_2}{\bar{Q}_1} \right)^2 \right) \quad (11)$$

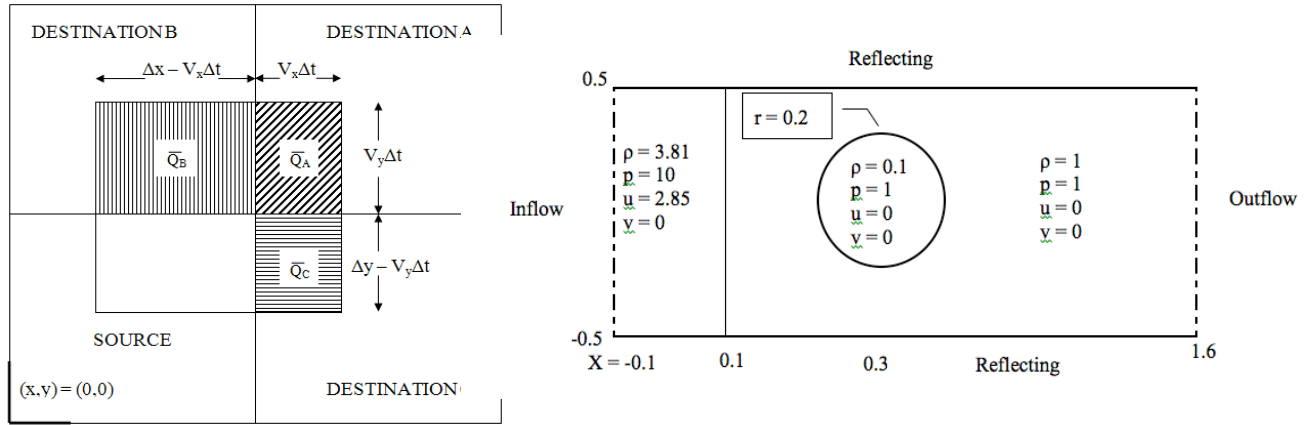


FIGURE 2. [Left] Two dimensional motion of a single QDS particle showing “sub-particle” contributions. [Right] The initial conditions for the two dimensional shock bubble interaction problem.

2D General Reconstruction and Implementation

Multi-dimensional extension is performed using the same principles applied for a single dimensional reconstruction. The variation of conserved quantity $Q(x,y)$ over two dimensional space is assumed to be:

$$\begin{aligned}
 Q(x,y) = & Q_{eff} + \left(\frac{dQ}{dx}\right)(x - 0.5\Delta x) + \left(\frac{d^2Q}{dx^2}\right)\frac{(x - 0.5\Delta x)^2}{2} \dots + \left(\frac{d^{n-1}Q}{dx^{n-1}}\right)\frac{(x - 0.5\Delta x)^{n-1}}{(n-1)!} \\
 & + \left(\frac{dQ}{dy}\right)(y - 0.5\Delta y) + \left(\frac{d^2Q}{dy^2}\right)\frac{(y - 0.5\Delta y)^2}{2} \dots + \left(\frac{d^{n-1}Q}{dy^{n-1}}\right)\frac{(y - 0.5\Delta y)^{n-1}}{(n-1)!}
 \end{aligned} \tag{12}$$

The subsequent (effective) cell centered value of Q is:

$$Q_{eff} = Q_r - \frac{\Delta x^2}{24} \left(\frac{d^2Q}{dx^2}\right) - \frac{\Delta x^4}{1920} \left(\frac{d^4Q}{dx^4}\right) \dots - \frac{2\Delta x^{n-1}}{n!} \left(\frac{1}{2}\right)^n \left(\frac{d^{n-1}Q}{dx^{n-1}}\right) - \frac{\Delta y^2}{24} \left(\frac{d^2Q}{dy^2}\right) - \frac{\Delta y^4}{1920} \left(\frac{d^4Q}{dy^4}\right) \dots - \frac{2\Delta y^{n-1}}{n!} \left(\frac{1}{2}\right)^n \left(\frac{d^{n-1}Q}{dy^{n-1}}\right) \tag{13}$$

Following this, the average value of conserved quantity in the region bound by $[xL, yL] - [xR, yR]$ is required:

$$\begin{aligned}
 \bar{Q} = & \frac{1}{(xR - xL)(yR - yL)} \int_{yL}^{yR} \int_{xL}^{xR} Q(x) dx dy \\
 = & Q_{eff} \\
 & + \frac{1}{(xR - xL)} \left[\left[\left(\frac{dQ}{dx}\right)\frac{(xR - 0.5\Delta x)^2}{2} \dots + \left(\frac{d^{n-1}Q}{dx^{n-1}}\right)\frac{(xR - 0.5\Delta x)^{n-1}}{n!} \right] - \left[\left(\frac{dQ}{dx}\right)\frac{(xL - 0.5\Delta x)^2}{2} \dots + \left(\frac{d^{n-1}Q}{dx^{n-1}}\right)\frac{(xL - 0.5\Delta x)^{n-1}}{n!} \right] \right] \\
 & + \frac{1}{(yR - yL)} \left[\left[\left(\frac{dQ}{dy}\right)\frac{(yR - 0.5\Delta y)^2}{2} \dots + \left(\frac{d^{n-1}Q}{dy^{n-1}}\right)\frac{(yR - 0.5\Delta y)^{n-1}}{n!} \right] - \left[\left(\frac{dQ}{dy}\right)\frac{(yL - 0.5\Delta y)^2}{2} \dots + \left(\frac{d^{n-1}Q}{dy^{n-1}}\right)\frac{(yL - 0.5\Delta y)^{n-1}}{n!} \right] \right] \tag{14}
 \end{aligned}$$

Since the average requires bounding regions in both translational directions, application of splitting (as applied to TDEFM to improve computational efficiency) is impossible and the full N^2 number of particles (i.e. 9 when 3 particles are used per direction, 16 for 4 etc.) are required for a complete flux computation. Previous extensions required only $2N$ particles. Unlike the one dimensional reconstruction, each particle carries three separate fluxes (for three difference destination cells) and so any single QDS particle possesses three “sub-particles” based on different integral bounds. This concept is demonstrated in Figure 2 showing each unique sub-region (A – C).

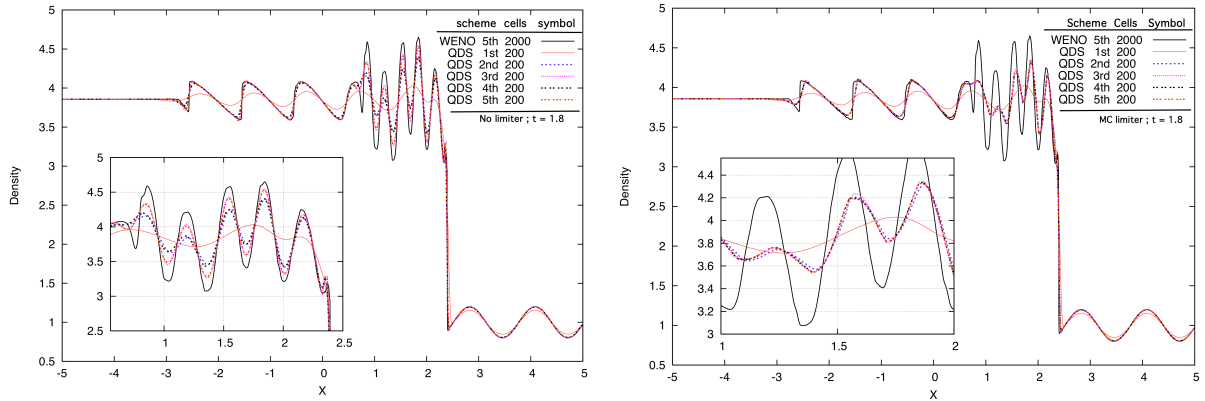


FIGURE 3. Density profile of the shock-acoustic-wave case at $t = 1.8$. The solid black line is WENO-3 (fifth order) with 2000 cells compared with QDS scheme using 200 cells without slope limiting [left] and using a MC (Monotonized central) limiter [right] from 1st order to 5th order.

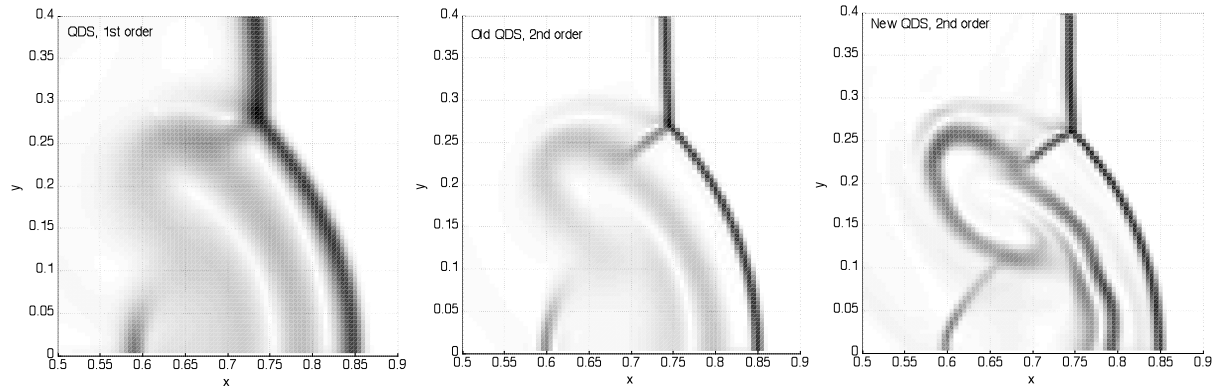


FIGURE 4. Results at $t = 0.2$ s for the 2D shock/bubble interaction problem for QDS using 340×100 cells. [Left] QDS, 1st order, [Middle] 2N QDS, 2nd order, [Right] Proposed N² QDS, 2nd order. All solutions use the same kinetic CFL number and the MC limiter applied to slopes prior to reconstruction.

RESULTS

One Dimensional Shock/Acoustic wave interaction problem

An ideal test case for testing the general one dimensional extension of QDS is the interaction of a Mach 3 shock with an acoustic wave as proposed by Shu and Osher [9]. The initial conditions are:

$$(\rho, v, P) = \begin{cases} (3.857143, 2.629369, 10.333333) & x < -4, \\ \left(1.0 + \frac{1}{5} \sin 5x, 0.0, 1.0\right) & -4 \leq x. \end{cases} \quad (15)$$

Results for various QDS configurations with 200 cells are shown in Figure 3 compared to a WENO benchmark employing 2000 cells. The improvement due to extension from first to second order is most significant with further higher orders offering only slight improvements over the second order extension. The general trend is in agreement with the WENO benchmark with third order QDS solutions resulting in similar levels of dissipation to a 5th order WENO solution (not shown).

2D simulation: Shock-bubble interaction

The strength of correct multi-dimension reconstruction is demonstrated in two dimensions for the shock/bubble interaction problem [10]. The initial conditions for the problem are shown in Figure 2. Numerical schlierens (showing gradients of density) are presented in Figure 4 for various QDS configurations on a very coarse grid (340×100 cells). The increase in resolution from first to second order is significant regardless of method – however,

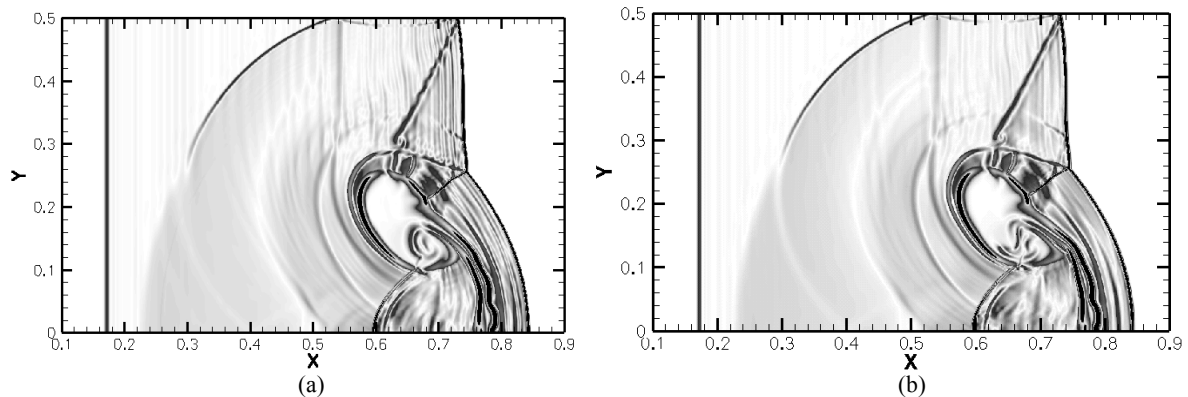


FIGURE 5. Zoom of shock-bubble Schlieren image with 1700x500 cells at time 0.2. QDS 3rd scheme using (a) 3 particles, (b) 4 particles with MC limiter.

application of correct multi-dimensional reconstructions results in higher resolution of the circulation and reflected shock located at $x = 0.6$. Results for larger grid resolutions are shown in Figure 5 for both 3 and 4 QDS particles employed per direction using the MC limiter.

CONCLUSION

The Quiet Direct Simulation (QDS) method has been presented with a general method for extension of spatial accuracy using multi-dimensional reconstruction. The results shown demonstrate an improved resolution in one dimension for higher orders of accuracy (up to 5th order) and even further improvement resulting from the correct multi-dimensional extension. The increase in resolution, specifically in two or three dimensional simulations, comes at the cost of additional computational expense. However, the speed of the QDS method, already significantly faster than many existing Finite Volume Methods (FVMs), still allows the N^2 general extension to higher order to compete with existing, lower dissipation methods.

ACKNOWLEDGMENTS

We would like to thank Dr. Matthew Smith of the National Center for High-Performance Computing in Taiwan and the National Science Council of Taiwan for the support of the corresponding author, Prof. J.-S. Wu, through Grant NSC-99-2922-I-009-107.

REFERENCES

1. G.A. Bird, *Molecular Gas Dynamics and the Direct Simulation of Gas Flows*, Clarendon Press, Oxford, 1994.
2. D.I. Pullin, Direct simulation methods for compressible inviscid ideal gas flow, *J. Comp. Phys.* 34: pp. 231-244, 1980.
3. M.R. Smith, M. N. Macrossan, M. M. Abdel-Jawad, Effects of direction decoupling in flux calculation in finite volume solvers, *J. Comp. Phys.*, 227:pp. 4142-4161, 2008.
4. B.J. Albright et al. Quiet direct simulation of Eulerian fluids, *Phys.Rev.E*, 65: pp.1-4, 2002.
5. M.R. Smith, H.M. Cave, J.-S. Wu, M.C. Jermy, Y.-S. Chen, An improved Quiet Direct Simulation method for Eulerian fluids using a second-order scheme, *J. Comp. Phys.*, 228:pp. 2213–2224, 2009.
6. M.N. Macrossan, The Equilibrium Flux Method for the calculation of flows with non-equilibrium chemical reactions, *J. Comp. Phys.*, 80[1]:pp. 204-231, 1989.
7. M.R. Smith, “*The true direction equilibrium flux method and its application*”, PhD Thesis, University of Queensland, Australia, 2008.
8. Juan-Chen Huang, Heng Lin, Jaw-Yen Yang, Implicit preconditioned WENO scheme for steady viscous flow computation, *J. Comp. Phys.* 228:pp. 420-438, 2009.
9. C.-W. Shu, S. Osher, Efficient implementation of essentially non-oscillatory shock-capturing schemes, *J. Comp. Phys.*, 77: pp. 439–471, 1988.
10. Cada, M., Torrilhon, M., Compact third-order limiter functions for finite volume methods, *J. Comp. Phys.*, 228: pp. 4118-4145, 2009.